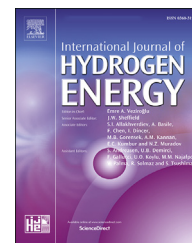




ELSEVIER

Available online at [www.sciencedirect.com](http://www.sciencedirect.com)

ScienceDirect

journal homepage: [www.elsevier.com/locate/ijhe](http://www.elsevier.com/locate/ijhe)

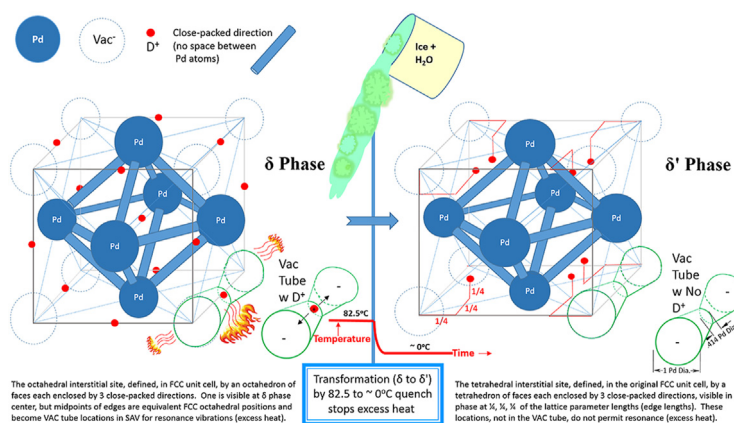
# The role of superabundant vacancy delta to delta prime transformation in stopping Fleischmann-Pons heat effect in palladium-deuterium

M.R. Staker <sup>a,b,\*</sup><sup>a</sup> Department of Engineering, Loyola University Maryland, 4501 North Charles St, Baltimore, MD, 21210, USA<sup>b</sup> American Patent Institute, 2817 Wesleyan Drive, Churchville, MD, 21028, USA

## HIGHLIGHTS

- The revised phase diagram of the Palladium - Deuterium system is employed.
- Delta phase of the Super Abundant Vacancy phases (SAV) is key.
- Phase transformation stops excess heat in a Low Energy Nuclear Reaction.
- Measurement of delta to delta prime phase transition is made by calorimetry.
- A quench heat treatment initiates delta to delta prime phase transition.

## GRAPHICAL ABSTRACT



## ARTICLE INFO

## Article history:

Received 15 November 2022

Received in revised form

24 December 2022

Accepted 1 January 2023

Available online xxx

## Keywords:

Cold fusion

Low energy nuclear reactions (LENR)

Fleischmann-pons heat effect

Nuclear active environment (NAE)

## ABSTRACT

A calorimeter, designed for electrolysis of Pd in heavy water, capable of measuring heat and power output with a precision of  $\pm 0.5\%$ , was used to determine changes in output during a compulsory quick-drop in temperature. The change in temperature was forced on the electrolysis cell while it was producing nuclear energy at excess power levels of 240 W/cm<sup>3</sup> and after producing a continuous excess heat amount of 150 MJ/cm<sup>3</sup> (14 000 eV/atom of Pd). The temperature change (from 82.5 °C to  $\sim 0$  °C) resulted in a total loss of excess power (nuclear power) and indicates the regions of the microstructure that were ordered superabundant vacancy (SAV) phase transformed from  $\delta$  to the ordered superabundant vacancy phase  $\delta'$ . The  $\delta$  phase is responsible for producing excess heat and power while the  $\delta'$  phase produces no excess heat or power. Deuterium in the  $\delta$  phase occupies the octahedral sites but occupies the tetrahedral sites in the  $\delta'$  phase. In either case,  $\delta$  and  $\delta'$  are minor phases with volume fractions in the two-phase microstructure of approximately

\* Corresponding author.

E-mail address: [m.r.staker@alum.mit.edu](mailto:m.r.staker@alum.mit.edu).<https://doi.org/10.1016/j.ijhydene.2023.01.001>0360-3199/© 2023 The Author(s). Published by Elsevier Ltd on behalf of Hydrogen Energy Publications LLC. This is an open access article under the CC BY-NC-ND license (<http://creativecommons.org/licenses/by-nc-nd/4.0/>).

Palladium-deuterium phase diagram  
Phase transition controls nuclear energy

0.03 and 5.0 percent for  $\delta$  and  $\delta'$ , respectively. This evidence of termination of excess power supports previous indications in the literature of such a transformation.

© 2023 The Author(s). Published by Elsevier Ltd on behalf of Hydrogen Energy Publications LLC. This is an open access article under the CC BY-NC-ND license (<http://creativecommons.org/licenses/by-nc-nd/4.0/>).

## Introduction

Both delta and delta prime ( $\delta$  and  $\delta'$ ) phases in palladium (Pd) deuteride (D) are ordered superabundant vacancy (SAV) phases with compositions and structures of  $\text{Pd}_3\text{Vac}_1\text{D}_x$  [1–16] where  $x$  is 4–8, depending on the D activity. This structure, originally face centered cubic (FCC), becomes simple cubic (SC) with the introduction of ample D or hydrogen (H) and an active source of vacancies (VAC). In this ordered state, VAC occupy the eight corners while Pd occupies the six face-centered positions of the original FCC unit cell [13]. Delta and delta prime phases result from hydrogen-induced vacancy formation [1,4a,15–36] at high temperature and pressure or at ambient conditions: it has been proposed that VAC are produced during room temperature electrolysis by a dislocation mechanism involving dragging edge jogs connected between screw dislocations, followed by VAC relocation (attracted to D+ during electromigration) to the corners of the original FCC unit cell [13]. These SAV unit cells are only possible because of the long range order that develops when the atom fraction of VAC becomes about 33% with a reduction in free energy due to long range order. VAC distributed at random unit cell positions (including both corners and face-centered) have higher free energy than when the VAC become ordered (occupying only the unit cell corner positions). SAV  $\delta$  or  $\delta'$  would not be possible if there was no long range order, even if the atomic fraction were 33%. Screw dislocation intersections during plastic deformation form these edge jogs, and strings of VAC are created in the wake of these moving edge jogs because their Burgers vectors are perpendicular to motion [13,15,36–38a]. Thus, plastic deformation is essential in creating SAV phases at room temperature and is provided by using cold worked Pd and enhanced further initially (at the start of electrolysis) by multiple loadings and unloadings of D by reversing electrolysis polarity multiple times, causing multiple trips through the alpha ( $\alpha$ ) plus beta ( $\beta$ ) miscibility gap and the associated plastic deformation [13]. This mechanism provides for the formation of SAV phases near room temperature in spite of VAC diffusion being too slow. Each stint of unloading and reloading D preserves most of the previously created VAC, allowing the VAC concentration to ratchet up with each trip through the miscibility gap [15]. A quantitative estimate [14] of the volume fraction of VAC needed for  $\delta$  phase (or even  $\delta'$ ) by this mechanism, shows diffusion of vacancies from the surface or from grain boundaries is not required in order to form these phases at room temperature (Appendix B of Ref. [13]). In addition, Fukai [4a] reveals that: “this structure [ $\text{M}_3\text{VacH}_4$ ], once formed under high  $p_{\text{H}}$ , T [pressure, temperature] conditions, remains stable after recovery to ambient conditions.” Here M is a variety of metals [13]. The subject of this research is the shifting of H or D in  $\text{M}_3\text{VacD}_4$  from

octahedral to tetrahedral sites (or vice versa) while the ordered SC shell remains otherwise essentially unchained except for the increased negative charge on the VAC [12] (see next section).

Pitt and Gray [39] and Ferguson et al. [40] have measured the hydrogen (or deuterium) in Pd-D (or Pd-H) in octahedral sites near room temperature, with a shift to tetrahedral sites at lower temperature. It has been suggested [12–15] that excess heat (more heat produced than is put in by electrolysis) during Low Energy Nuclear Reactions (LENR), or Lattice Assisted Nuclear Reactions (LANR), in Pd-D occurs when deuterium occupies octahedral interstitial sites ( $\delta$ ) rather than tetrahedral sites ( $\delta'$ ). Further, changes in resistivity [13,14] strongly suggested spontaneous transformations of some  $\delta$  phase to  $\delta'$  (or new  $\delta'$  formation) during excess heat. Since the proposed new phase diagram for Pd-D (shown in Fig. 1) shows  $\delta$  phase is present near room temperature and higher, while  $\delta'$  phase is present at lower temperatures, it is instructive to see if the production of excess (nuclear) power and heat (or termination thereof) would correlate to this transition in temperature (lowering) and the accompanying phase change. Much has been learned about the conditions necessary to start [15] the Fleischmann-Pons heat effect in Pd-D (i.e. LENR or LANR), but more can also be learned about the mechanism from implementing conditions to stop the Fleischmann-Pons heat effect.

## Materials and experimental methods

Complete experimental details of the calorimeter are in Ref. [13], however Pd/D<sub>2</sub>O (active) and Pt/H<sub>2</sub>O (control) electrolytic cells, for electrolysis of Pd in heavy water with 0.5 M LiOD are shown in Fig. 2. The present research uses the same methods and materials of previous papers [13–15] including calibrations before and after the experiment. In these prior publications [13–15], it was shown that excess power (nuclear) persisted continuously for 46 days at levels from 20 to 240 Watts/cm<sup>3</sup> and these power levels integrated to excess heat amounting to 150 MJ/cm<sup>3</sup> (14 000 eV/atom of Pd). After the electrolysis was run for 46 days, the excess power was at a level of 240 Watts/cm<sup>3</sup> and a temperature of 82.5 °C. The calorimeter box was quickly opened, and a pre-prepared 8 L bucket of ice-water mixture at approximately 0 °C was placed under the Pd/D<sub>2</sub>O cell and quickly raised, surrounding and immersing the cell to just below the Teflon stops. The monitored (measured) temperature in the cell quickly approached 0 °C. After thermal equilibrium was achieved (just above 0 °C), the bucket was held in place for a further 15 min; then the bucket was removed and the continually operating cell was allowed to return to its operating temperature prior to emersion. This, however, was not the same temperature of 82.5 °C (with excess power), but

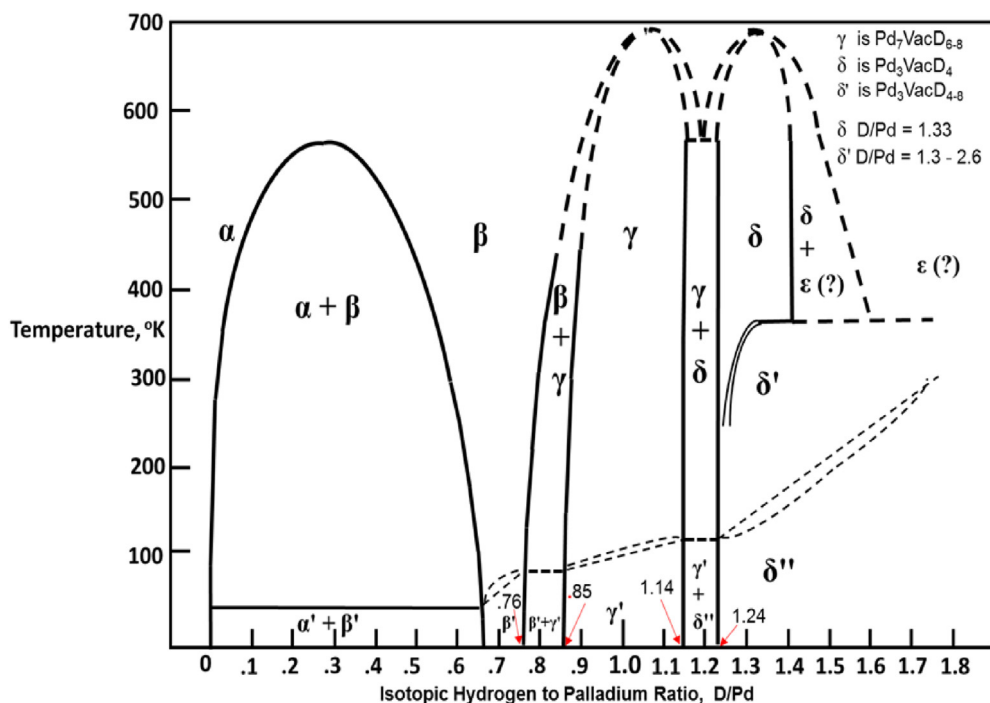


**Fig. 1 – Equilibrium Phase Diagram for Hydrogen – Palladium [13–15] with SAV delta phase from 1.14 to >1.4 D/Pd ratio. In the two-phase field ( $\gamma + \delta$ ), the D/Pd ratio ranges from 1.14 to 1.24. Delta and Delta prime are stoichiometric at 1.33, but range from 1.24 to 1.42 ( $\delta$ ) or 2.66 ( $\delta'$ ).**

rather the calibrated temperature without excess power for that input power level. Then a calibration check was run, confirming that the cell had returned to its calibration level of input power and delta temperature,  $\Delta T$  (difference between cell interior and surrounding air temperature inside the box of the calorimeter). The cell temperature and input powers were monitored for another 30 days.

## Results and discussion

During the 30 days after emersion (quench), the monitored cell did not produce any further excess power or heat. It stayed on the calibration curve of delta temperature ( $\Delta T$ ), absent excess power, vs input power. This can be seen from Table 1. This also verified that there was no shift in the calibration of the cell during the 76 days of operation.

These results reveal that a sudden forced lowering of the temperature of the Pd-D cathode by about 82 °C stopped excess power and heat (nuclear power and heat), even though it was still under electrolysis and still loaded with high fugacity D. Resistivity measurements, using the same methodology previously reported in prior papers [13–15] of the experimental correlation between measured resistance and D/Pd ratio, indicated the Pd cathode remained loaded to the same activity level (approximate average bulk D/Pd ratio of 0.93) as that prior to emersion. As will be seen below, this produced a violation of the conditions necessary for achieving the Fleischmann-Pons heat effect [15].

Delta and delta prime are minor SAV micro-constituents in a two-phase microstructure in the Pd-D cathode with

previously assessed [14] volume fractions of 0.03 and 5.0 percent for  $\delta$  and  $\delta'$ , respectively. It is suggested that this heat treatment results in a shift of the deuterons from the octahedral sites to the tetrahedral sites, corresponding to the  $\delta$  to  $\delta'$  phase transformation (Figs. 1 and 3), supportive of a prediction [14] from the literature:

“It has been understood that  $\delta$  phase, with interstitial occupancy at octahedral sites, is more probable than  $\delta'$  phase with interstitial occupancy at tetrahedral sites near room temperature. This is possibly true for the lower D/Pd ratios ( $r_x$ ). However at high  $r_x$ , this research [14], along with other research [29,32,34,39–41], suggests the reverse (tetrahedral more likely) since the volume fraction of  $\delta'$  (5.0%) is much higher than the volume fraction of  $\delta$  (.03%). Isaeva et al. [29] has indicated the phase change to tetrahedral site occupancy is a change with more order than that of octahedral site occupancy: tetrahedral site is favored by having more order.”

In this shift, the distance from the center of the deuteron to the center of the VAC changes from  $a_o/2$  (in  $\delta$ ) to  $a_o \cdot \sqrt{3}/4$  (i.e.  $0.433 \cdot a_o$  in  $\delta'$ ) where  $a_o$  is the lattice parameter (see Fig. 3). Not all tetrahedral sites would be filled in the initial transition without additional deuterons moving in. In  $\delta$  there are 6 nearest neighbor deuterons (to the VAC) which are each shared by two VAC<sup>-</sup> (one on either side of the deuteron) giving an effective nearest neighbor count of 3 deuterons per VAC<sup>-</sup> (1 deuteron at  $1/2, 1/2, 1/2$  is surrounded by only Pd atoms, see Fig. 3). But in  $\delta'$ , the VAC<sup>-</sup> has 4 unshared nearest neighbor deuterons per VAC<sup>-</sup> (without additional deuterons moving in, or

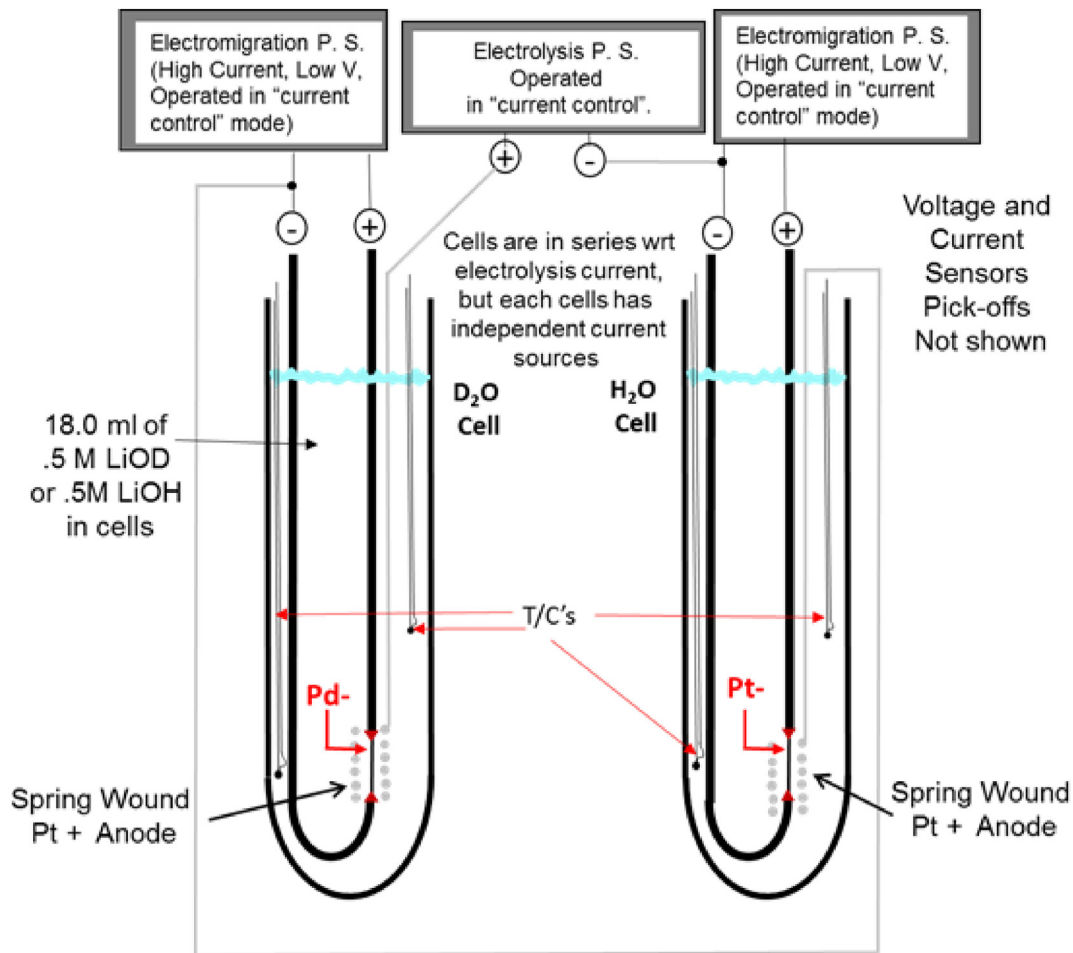


**Fig. 2 – Electrolytic cells of four nested (not shown) Pyrex test tubes [13] with Pd or Pt cathodes and Pt anodes, sealed with Teflon tops (not shown). Cells are in series on one “current controlled” power supply (P. S.). Independent electromigration currents from P. S.’s for each cell were operated in “current control” mode. The left cell (Pd cathode) has 18 ml of 0.5 M LiOD and the right cell has 18 ml of 0.5 M LiOH, from Refs. [13–15].**

potentially 8, if additional deuterons move in to fill all the tetrahedral sites), at a closer distance, creating a more negative charge [12] on the  $VAC^-$  (to balance local charge from the deuterons). It is suggested that this negative charge on the  $VAC^-$ , which is supplied by a slight localization of the conduction band electrons, also serves to lower the free energy state of the system since binding between  $VAC^-$  and  $D^+$ s is stronger due to a shorter distance and the higher numbers of  $D^+$ s per  $VAC^-$ .

Mixed amounts of tetrahedral and octahedral occupancy have been previously observed [39,40]. Remarkably, density functional theory (DFT) calculations for PdH at  $r_x = 1.0$  by Setayandeha et al. [42] found mixed octahedral and tetrahedral occupancy was the only result that would bring the partial atomic volume of hydrogen  $v_H$  into agreement with experiment, indicating PdH must contain 15–20% tetrahedral H with the remaining H in octahedral sites. Akiba [43] used the Rietveld analysis to show that 30% of D atoms are in

**Table 1 – Experimental conditions (ambient temperature = 23 °C).**

| State                    | D/Pd ratio | Temperature of Cell (°C) | Condition of Pd-D Cathode                | Result (Excess heat and power?)               | Reference       |
|--------------------------|------------|--------------------------|--|---|-----------------|
| prior to quench          | 0.93       | 82.5                     | $\beta + 0.03\% \delta + 5.00\% \delta'$ | excess heat + 240 W/cm <sup>3</sup> ex. Power | this work,13,14 |
| at quench                | 0.93       | dropping                 | transitioning                            | transitioning                                 | this work       |
| 0–15 min after quench    | 0.93       | ~0                       | $\beta + 5.03\% \delta'$                 | no excess power                               | this work,14    |
| After 15 min             | 0.93       | rising                   | $\beta + 5.03\% \delta'$                 | no excess power                               | this work,14    |
| during 30 d after quench | 0.93       | 42 to 45                 | $\beta + 5.03\% \delta'$                 | no excess power                               | this work,14    |
| calibration              | 0.93       | 45                       | $\beta + 5.03\% \delta'$                 | on calibration                                | this work,14    |

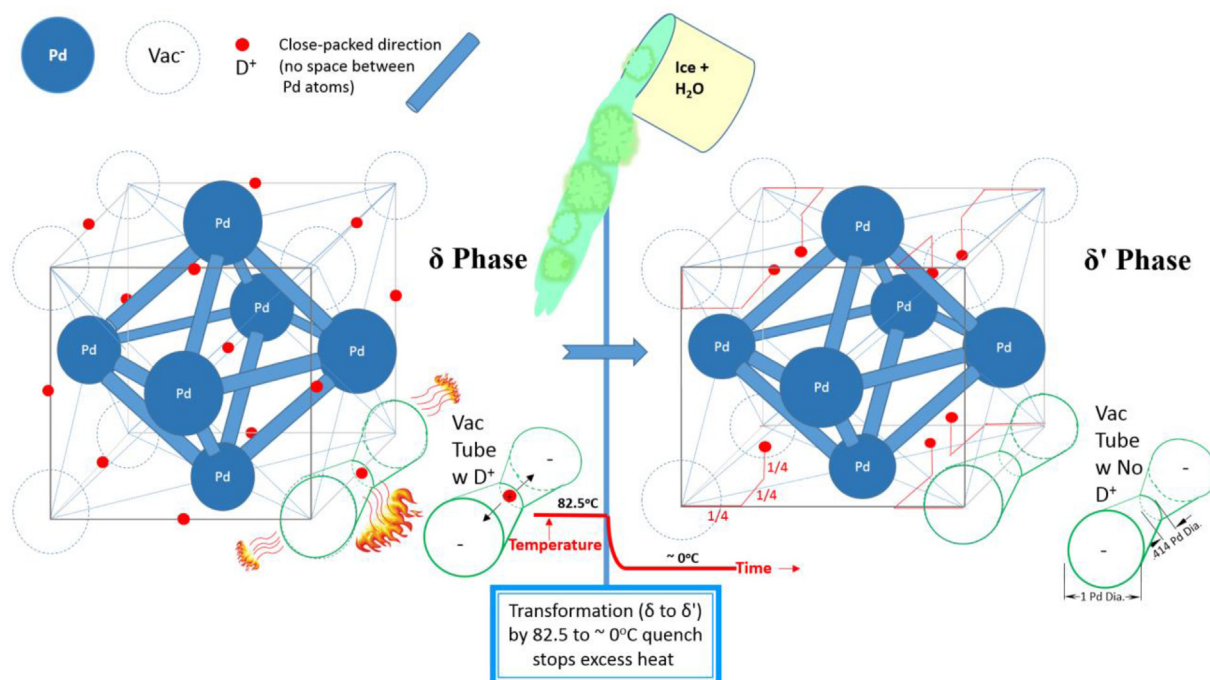


**Fig. 3 – The transformation of  $\delta$  phase, with D<sup>+</sup> at octahedral sites, to  $\delta'$  phase, with D<sup>+</sup> at tetrahedral sites. The octahedral interstitial site, defined, in the FCC unit cell, by an octahedron of 8 faces each face bounded by 3 close-packed directions. At the left, one is visible at  $\delta$  phase center, but midpoints of FCC edges are equivalent FCC octahedral positions and become VAC tube locations in SAV for resonance vibrations (excess heat). The tetrahedral interstitial site, defined, in the original FCC unit cell, by a regular tetrahedron of 4 faces each bounded by 3 close-packed directions, visible in  $\delta'$  phase at  $1/4, 1/4, 1/4$  of the lattice parameter (FCC edges). Unit cell face diagonals are also close-packed directions and each tetrahedron includes 3 half-diagonals. These tetrahedral interstitial sites are not in the VAC tube and therefore do not enable resonance vibrations (excess heat).**

tetrahedral sites while 70% are in octahedral sites. Several other researchers using Pd and its alloys with gold (Au) also found partial occupancy of tetrahedral sites by D. Also, by quickly quenching PdD, formed by loading with deuterium at elevated temperature, Syed et al. [44] measured a noteworthy increase in the temperature of superconductivity  $T_c$  to about 60° kelvin. This assents to previous results [14] showing that a partial  $\delta$  to  $\delta'$  transformation spontaneously occurred (or at least more  $\delta'$  formed in addition to the existing combination of  $\delta + \delta'$ ) during the production of excess heat; and it was concluded that the  $\delta'$  portion (phase) had very low resistivity. This low resistivity suggested [45] a possible link between LENR, SAV and superconductivity. Complementarily, Mayer [46] has proposed that LENR is initiated in a phase-transition yielding a fraction of the electrons as superconducting electrons via Cooper pairs, which then start a deuteron-driven chain of nuclear reactions.

However, once transformation has proceeded completely to  $\delta'$ , this SAV phase in Pd-D is now in a lower free energy state as can be seen from the stronger bond as explained above and also supported by Bukonte et al. [32] and will need additional activation energy to force the deuterons back into the octahedral sites ( $\delta$  phase). Occupation of either octahedral or tetrahedral (with temperature dependence) and a high VAC concentration is consistent with the astute recognition and statement of Fukai [4b]:

“... most important implication in the physics of SAV is that the most stable structure of all M – H alloys is in fact the defect structure containing a large number of M-atom vacancies. All M – H alloys should tend to assume such defect structures, ordered or disordered depending on the temperature, as long as the kinetics allows. *In practice, however, M–H alloys are in most cases prepared under conditions where M-atom vacancies cannot be introduced.* Thus it can be said that most (all) phase diagrams of M – H systems reported to date are metastable ones. These metastable diagrams are certainly useful as such, but the recognition that they are metastable ones is of basic importance. The real equilibrium phase diagrams including M-atom(s) vacancies have not been obtained so far.” [emphasis added]

Tetrahedral site occupancy has more order and lower free energy [32]. Increasing temperature and coaxing deuterons back into octahedral sites, agrees with (and explains) reported [47–52] “positive feedback” (an increase in temperature produces more excess power which increases the temperature further and so on). But, if all previously available VAC (originally scattered throughout the  $\beta$ -phase) become locked in the  $\delta'$  phase, it would be necessary to create more VAC in order to form any new  $\delta$  phase near room temperature. A total shift of all  $\delta$  to  $\delta'$  would produce violations of rules number 1 and 4 of the essential criteria for achieving the Fleischman-Pons heat

effect [15]: (1) a highly available VAC concentration and (4) existence of  $\delta$  phase; and thus make excess heat implausible. Creating new VAC near room temperature requires new plastic deformation (since diffusion is too slow). A way to introduce added plastic deformation would be by multiple reversals of polarity of the electrolysis (unload D anodically followed by cathodically reloading), thus transitioning the  $\alpha + \beta$  miscibility gap multiple times, as was done at the beginning of this experiment [13–15]. In addition, the crystallography of the  $\delta'$  phase with the deuterons at tetrahedral sites does not allow for resonance conditions that allow large vibrations of the deuterons and a nuclear active environment necessary for the production of excess heat and power [12,15]. A review of conditions was recently published [53]. The green tubes running along all 12 edges of the unit cell (Figs. 3 and 4) are the locations of deuteron longitudinal vibrations (arrows) and resonance during excess heat in  $\delta$ . These VAC tubes are empty tubes except for strings of deuterons with spacing equal to the lattice parameter and are a result of the unique lattice geometry of SAV  $\delta$  phase shown in Fig. 3 Of Ref. [12] where both lattices of beta ( $\beta$ ) deuteride of Pd–D and  $\delta$  of Pd<sub>3</sub>VacD<sub>4</sub> line up in the [100], [010] and [001] directions. The vacancy channel (green tube) is shown with a varying diameter of between 0.414 and 1.0 of that of the Pd atom diameter ( $2.75 \times 10^{-10}$  m). The Pd atoms at the end of each tube (from  $\beta$  deuteride) supply the driving force for the resonance condition from the force available through Hooke's law (see Ref. [12]). The driving force comes from the normal thermal vibration of the Pd atom at its own natural

vibration frequency of 5.7 THz [12]. The D<sup>+</sup> ions vibrate inside these (green) tubes. These resonances have amplitudes exceeding unit cell dimensions (Fig. 4) and high velocities [12] raising the likelihood of nuclear interactions. These displacements also produce phonons from a quantum mechanical perspective. However, this is not possible if there are no deuterons (Fig. 3 and Fig. 4 insert) in the  $\delta'$  tubes (referred to as vacancy channels [12], lattice tubes [13] or empty undulating diameter tubes [14]). Inability to revert back to  $\delta$  phase is an example of sluggish kinetics (for the production of VAC) which bars achievement of phase diagram equilibrium conditions for  $\delta$ . A classic example of meta-stability is as-quenched martensite (with trapped interstitial carbon) where kinetics prevent the achievement of equilibrium phases of ferrite and free carbon (graphite). Apparently, heating a SAV phase promotes D-jumps from tetrahedral to octahedral sites and production of excess heat, while cooling a SAV phase promotes D-jumps to tetrahedral sites and absence of excess heat.

From the phase diagram (Fig. 1), the production of  $\delta$  phase requires, at least a local D/Pd ratio,  $r_x$ , of 1.14 (see the lever rule in Fig. 3 of Ref. [15]), and available VAC. If  $r_x < 1.14$ , locally and globally, or VAC content is too low (and cannot be introduced), SAV  $\delta$ -phases will not form, barring excess heat. In gas loading (without electrolysis and electromigration), or even if done via electrolysis, but with only minor electromigration [14], where bulk loading reaches merely  $r_x \sim 1.0$ , SAV  $\delta$ -phase would not form because (at least) the local  $r_x$  (enhanced by electromigration) needs to be  $\geq 1.14$  [15,38b]. If VAC concentration is

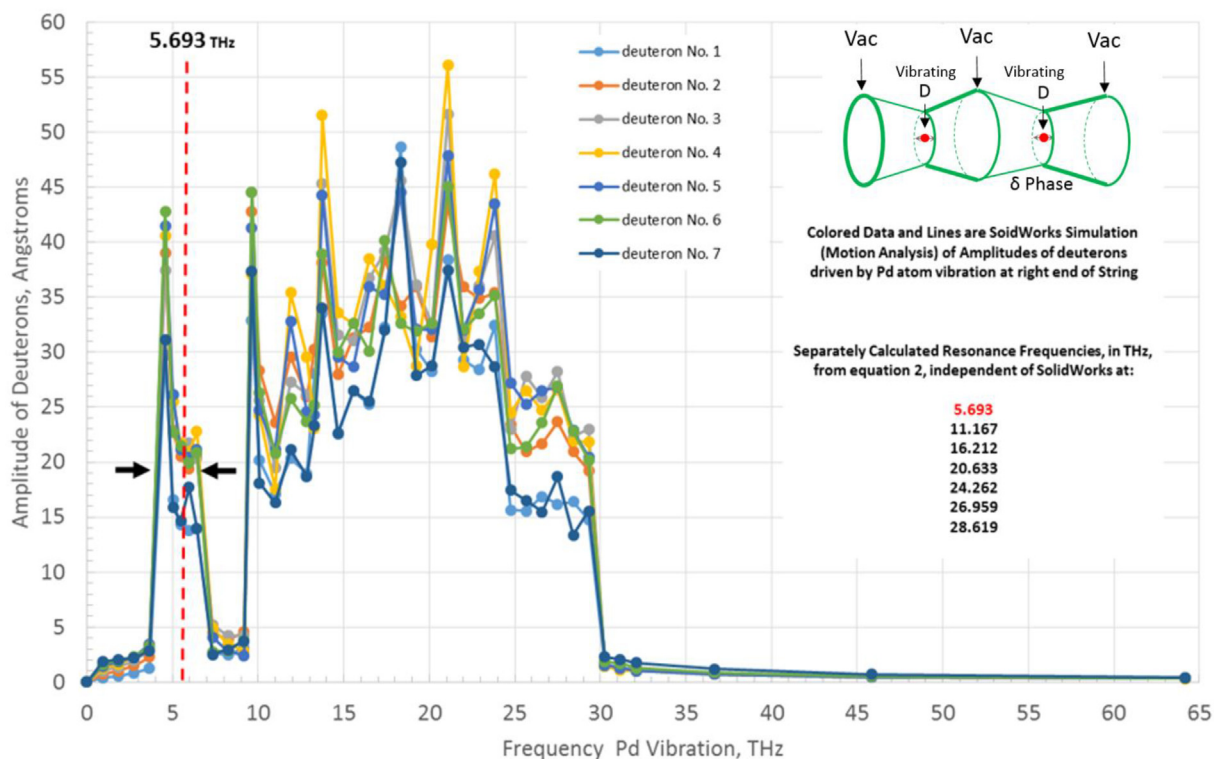


**Fig. 4 – Amplitude of vibrations of seven deuterons of SAV ( $\delta$  phase) due to Pd end atom at various frequencies, after Staker [12,15]. The first peak ( $m = 1$ , where  $m$  is mode number as defined in Ref. [12]) at 5.693 THz (approximate midpoint of half width) matches thermal vibration frequency of Pd (5.70 THz). If peak widths are taken into account, other peaks ( $2 \leq m \leq 7$ ) also match calculated resonance frequencies; but as  $m$  increases the peak widths overlap. Insert is the geometry of the vacancy tubes in  $\delta$  in which the deuterons vibrate.**

not limiting as during positive feedback (with activation energy for deuteron shift), the presence of  $\delta'$  can contribute to formation of  $\delta$ , since  $\delta'$  can act as a deuteron reservoir since there are twice as many tetrahedral as octahedral sites.

## Conclusions

The sudden forced temperature change during electrolysis of Pd (0.5 M LiOD in heavy water) from  $\sim 82.5$  °C to  $\sim 0$  °C while producing 240 W/cm<sup>3</sup> excess power and continuous excess heat of 150 MJ/cm<sup>3</sup> (14 000 eV/atom of Pd) resulted in a total loss of excess power; and indicates the regions of the microstructure of ordered superabundant vacancy (SAV) phase transformed from  $\delta$  to ordered superabundant vacancy  $\delta'$ . The  $\delta$  phase is responsible for producing excess heat and power while the  $\delta'$  phase produces no excess heat or power. Deuterium in the  $\delta$  phase occupies the octahedral sites, but it occupies tetrahedral sites in the  $\delta'$  phase. Delta and delta prime are minor (from a volume fraction perspective) SAV phases with previously estimated [14] volume fractions in the two-phase microstructure of approximately 0.03 and 5.0 percent for  $\delta$  and  $\delta'$ , respectively. This evidence of termination of excess power supports indications in the literature of such a transformation.

## Declaration of competing interest

The author declares that he has no known competing financial interests or personal relationships that could have appeared to influence the work reported in this paper.

## Acknowledgements

Without equipment and logistics support of Donald S. Hassett this research would not have been possible. Gratitude is expressed to S. Joseph and S. Anthony for their help. The author is grateful to Anthropocene Institute, Palo Alto, CA for covering the color printing cost and the article processing charge (APC) for this paper.

## REFERENCES

- [1] Fukai Y, Okuma YN. Evidence of copious vacancy formation in Ni and Pd under a high hydrogen pressure. *Jpn J Appl Phys* 1993;32:L1256–9. <https://doi.org/10.1143/JJAP.32.L1256>.
- [2] Oates WA, Wenzl H. On the copious formation of vacancies in metals. *Scripta Met. et Mat.* 1994;30(7):851–4. [https://doi.org/10.1016/0956-716X\(94\)90402-2](https://doi.org/10.1016/0956-716X(94)90402-2).
- [3] Oates WA, Wenzl H. On the formation and ordering of superabundant vacancies in palladium due to hydrogen absorption. *Scripta Met. et Mat.* 1995;33(2):185–93. [https://doi.org/10.1016/0956-716X\(95\)00159-S](https://doi.org/10.1016/0956-716X(95)00159-S).
- [4] Fukai Y. *The metal–hydrogen system: basic bulk Properties*. 2nd ed. Berlin: Springer; 2005.a)pp. 216–217,b)p. 225.
- [5] Fukai Y. Superabundant vacancies formed in metal–hydrogen alloys. *Phys Scripta* 2003;T103(2003):11. <https://doi.org/10.1238/Physica.Topical.103a00011>.
- [6] Degtyareva VF. Electronic origin of superabundant vacancies in Pd hydride under high hydrogen pressures, Presented on the Conference on Hydrogen Materials Science (ICHMS), Yalta, Ukraine. 25–31 August, <http://arxiv.org/pdf/1001.1525.pdf>. [Accessed 25 November 2018].
- [7] Tanguy D, Mareschal M. Superabundant vacancies in a metal–hydrogen system: Monte Carlo simulations. *Phys Rev B* 2005;72(17):174116. <https://doi.org/10.1103/PhysRevB.72.174116>.
- [8] Fukai Y. Hydrogen-induced superabundant vacancies in metals: implication for electrodeposition. In: Ochsner A, Murch GE, Delgado JMO \ Q, editors. *Defect and Diffusion Form* 312–vol. 315; 2011. p. 1106–15.
- [9] dos Santos DS, Miraglia S, Fruchart D. A high pressure investigation of Pd and the Pd–H system. *J Alloys Compd* 1999;291. [https://doi.org/10.1016/S0925-8388\(99\)00281-9](https://doi.org/10.1016/S0925-8388(99)00281-9). L1– L5.
- [10] Fukai Y, Okuma N. Formation of superabundant vacancies in Pd hydride under high hydrogen pressures. *Phys Rev Lett* 1994;73(12):1640–3. <https://doi.org/10.1103/PhysRevLett.73.1640>.
- [11] Fukada Y, Hioki T, Motohiro T. Multiple phase separation of super-abundant-vacancies in Pd hydrides by all solid-state electrolysis in moderate temperatures around 300 C. *J Alloys Compd* 2016;688:404–12. <https://doi.org/10.1016/j.jallcom.2016.07.176>.
- [12] Staker MR. A Model and simulation of lattice vibrations in a superabundant vacancy phase of Palladium-Deuterium. *Model Simul Mat Sci Eng* 2020;28:065006. <https://doi.org/10.1088/1361-651X/ab9994>.
- [13] Staker MR. Coupled calorimetry and resistivity measurements, in conjunction with an emended and more complete phase diagram of the Palladium - isotopic Hydrogen system. *J. Condensed Matter Nucl. Sci.* 2019;29:129–68. <https://www.lenr-canr.org/acrobat/StakerMRpreprintco.pdf>.
- [14] Staker MR. Estimating volume fractions of superabundant vacancy phases and their potential roles in low energy nuclear reactions and high conductivity in the Palladium–isotopic Hydrogen system. *Mater Sci Eng B* 2020;259:114600. <https://doi.org/10.1016/j.mseb.2020.114600>.
- [15] Staker MR. How to achieve the Fleischmann-Pons heat effect. *Int J Hydro Energy* 2023;48(5):1988–2000. <https://doi.org/10.1016/j.ijhydene.2022.10.070>. available online 1 Nov 2022).
- [16] Fukai Y, Okuma N. Formation of superabundant vacancies in Pd hydride under high hydrogen pressures. *Phys Rev Lett* 1994;73(12):1640–3. <https://doi.org/10.1103/PhysRevLett.73.1640>.
- [17] Fukada Y, Hioki T, Motohiro T. Multiple phase separation of super-abundant-vacancies in Pd hydrides by all solid-state electrolysis in moderate temperatures around 300 C. *J Alloys Compd* 2016;688:404–12. <https://doi.org/10.1016/j.jallcom.2016.07.176>.
- [18] Oates WA, Wenzl H. On the copious formation of vacancies in metals. *Scripta Met. et Mat.* 1994;30:851–4. [https://doi.org/10.1016/0956-716X\(94\)90402-2](https://doi.org/10.1016/0956-716X(94)90402-2).
- [19] Oates WA, Wenzl H. On the formation and ordering of superabundant vacancies in palladium due to hydrogen absorption. *Scripta Met. et Mat.* 1995;33:185–93. [https://doi.org/10.1016/0956-716X\(95\)00159-S](https://doi.org/10.1016/0956-716X(95)00159-S).
- [20] Fukai Y. Superabundant vacancies formed in metal–hydrogen alloys. *Phys Scripta* 2003;2003(T103):11. <https://doi.org/10.1238/Physica.Topical.103a00011>.
- [21] Fukai Y, Mizutani M. Phase diagram and superabundant vacancy formation in Cr–H alloys. *Mater Trans* 2002;43:1079–84. <https://doi.org/10.2320/matertrans.43.1079>.
- [22] Tanguy D, Mareschal M. Superabundant vacancies in a metal–hydrogen system: Monte Carlo simulations. *Phys Rev*

- B 2005;72(17):174116. <https://doi.org/10.1103/PhysRevB.72.174116>.
- [23] Fukai Y. In: Ochsner A, Murch GE, Delgado JMO \ Q, editors. Hydrogen-induced superabundant vacancies in metals: implication for electrodeposition. Defect and diffusion form, vols. 312–315. Trans Tech Publications Ltd.; 2011. p. 1106–15. <https://doi.org/10.4028/www.scientific.net/DDF.312-315.1106>.
- [24] dos Santos DS, Miraglia S, Fruchart D. A high pressure investigation of Pd and the Pd–H system. *J Alloys Compd* 1999;291. [https://doi.org/10.1016/S0925-8388\(99\)00281-9](https://doi.org/10.1016/S0925-8388(99)00281-9). L1–L5.
- [25] Degtyareva VF. Electronic origin of superabundant vacancies in Pd hydride under high hydrogen pressures. Presented Conference on Hydrogen Materials Science (ICHMS), Yalta, Ukraine August 2009;25–31. <http://arxiv.org/pdf/1001.1525.pdf>. [Accessed 9 August 2022].
- [26] Zhang C, Alavi A. First-principles study of superabundant vacancy formation in metal hydrides. *J Am Chem Soc* 2005;127:9808–17. <https://doi.org/10.1021/ja050475w>.
- [27] Fukai Y, Mizutani M, Yokota S, Kanazawa M, Miura Y, Watanabe T. Superabundant vacancy–hydrogen clusters in electrodeposited Ni and Cu. *J Alloys Compd* 2003;356–357:270–3. [https://doi.org/10.1016/S0925-8388\(02\)01270-7](https://doi.org/10.1016/S0925-8388(02)01270-7).
- [28] Fukai Y. Formation of superabundant vacancies in M–H alloys and some of its consequences: a review. *J Alloys Compd* 2003;356–357:263–9. [https://doi.org/10.1016/S0925-8388\(02\)01269-0](https://doi.org/10.1016/S0925-8388(02)01269-0).
- [29] Isaeva LE, Bazhanov DI, Isaev E, Ereemeev SV, Kulkova SE, Abrikosov I. Dynamic stability of Palladium hydride: an ab initio study. *Int J Hydrogen Energy* 2011;36:1254–8. <https://doi.org/10.1016/j.ijhydene.2010.06.130>.
- [30] Fukai Y, Sugimoto H. Formation mechanism of defect metal hydrides containing superabundant vacancies. *J Phys Condens Matter* 2007;19(43):436201. <https://doi.org/10.1088/0953-8984/19/43/436201>.
- [31] Sugimoto H, Fukai Y. Migration mechanism in defect metal hydrides containing superabundant vacancies. *Diffusion-fundamentals.org* 2009;11(102):1–2. <https://ul.qucosa.de/api/qucosa%3A13024/attachment/ATT-0/>.
- [32] Bukonte L, Ahlgren T, Heinola K. Thermodynamics of impurity-enhanced vacancy formation in metals. *J Appl Phys* 2017;121:045102. <https://doi.org/10.1063/1.4974530>.
- [33] Fukai Y, Sugimoto H. The defect structure with superabundant vacancies to be formed from FCC binary metal hydrides: experiments and simulations. *J Alloys Compd* 2007;446 – 447:474–8. <https://doi.org/10.1016/j.jallcom.2006.11.090>.
- [34] Nazarov R, Hickel T, Neugebauer J. Ab Initio study of H-vacancy interactions in FCC metals: implications for the formation of superabundant vacancies. *Phys Rev B* 2014;89:144108. <https://doi.org/10.1103/PhysRevB.89.144108>.
- [35] Fukai Y, Kurokawa Y, Hiraoka H. Superabundant vacancy formation and its consequences in metal hydrogen alloys. *J Jpn Inst Metals* 1997;61:663e670 (in Japanese), <https://www.osti.gov/etdweb/biblio/600210>.
- [36] Read Jr WT. *Dislocations in crystals*. New York, NY: McGraw-Hill; 1953.
- [37] Hayden W, Moffatt WG, Wulff J. *Structure and Properties of Materials, Vol. III*. Wiley, New York: Mechanical Behavior; 1965. p. 63–4.
- [38] Reed-Hill RE. *Physical metallurgy principles*. Princeton, NJ: D. Van Nostrand; 1964. (a) pp. 139–143, (b) p. 334.
- [39] Pitt MP, Gray ME. Tetrahedral occupancy in the Pd–D system observed by *in situ* neutron powder diffraction. *Europhys Lett* 2003;64(3):344–50. <https://doi.org/10.1209/epl/i2003-00187-x>.
- [40] Ferguson Jr GA, Schindler AI, Tanaka T, Morita T. Neutron diffraction study of temperature-dependent properties of palladium containing absorbed hydrogen. *Phys Rev* 1965;137(2A):A483–7. <https://doi.org/10.1103/PhysRev.137.A483>.
- [41] Sinha KP. High temperature superconductivity in Pd–[H (D)]X system. *Natl Acad Sci Lett (India)* 2006;29(No. 3&4):125–9. <https://doi.org/10.48550/arXiv.cond-mat/0509596>. : arXiv:cond-mat/0509596 [cond-mat.supr-con], <https://arxiv.org/abs/cond-mat/0509596>. [Accessed 9 August 2022].
- [42] Sadat Setayandeha Samaneh, Goulda Tim, Vaezb Aminollah, Keith McLennana, Armanetc Nicolas, Gray Evan. First-principles study of the atomic volume of hydrogen in palladium. *J Alloys Compd* 25 May 2021;864:158713. <https://doi.org/10.1016/j.jallcom.2021.158713>.
- [43] Akiba Hiroshi, Kofu Maiko, Kobayashi Hirokazu, Kitagawa Hiroshi, Ikeda Kazutaka, Otomo Toshiya, Yamamuro Osamu. Nanometer-size effect on hydrogen sites in palladium lattice. *J Am Chem Soc* 2016;138(32):10238–43. <https://pubs.acs.org/doi/10.1021/jacs.6b04970>.
- [44] Syed HM, Gould TJ, Webb CJ, MacA. Gray E. Superconductivity in palladium hydride and deuteride at 52–61 kelvin, (also H. M. Syed, Ph.D. thesis, School of Natural Sciences. Australia: Griffith University; 2016. <https://doi.org/10.48550/arXiv.1608.01774>.
- [45] Staker MR. *The link between superabundant vacancies, cold fusion, and superconductivity - 30<sup>th</sup> Anniversary Invited Lecture*. Baltimore: Engineering Club Seminar at Loyola University Maryland; 2019. April 12,.
- [46] Mayer FJ. Superconductivity and low-energy nuclear reactions. *Results Phys* 2019;12(March):2075–7. <https://doi.org/10.1016/j.rinp.2019.02.027>.
- [47] Fleischmann M, Pons S. Calorimetry of the Pd–D<sub>2</sub>O system: from simplicity via complications to simplicity. *Phys Lett* 1993;176:118–29. [https://doi.org/10.1016/0375-9601\(93\)90327-V](https://doi.org/10.1016/0375-9601(93)90327-V).
- [48] Szpak S, Mosier-Boss PA, Smith JJ. On the behavior of Pd deposited in the presence of evolving deuterium. *J Electroanal Chem* 1991;302:255–60. [https://doi.org/10.1016/0022-0728\(91\)85044-P](https://doi.org/10.1016/0022-0728(91)85044-P).
- [49] Szpak S, Mosier-Boss PA, Miles MH, Fleischmann M. Thermal behavior of polarized Pd/D electrodes prepared by co-deposition. *Thermochim Acta* 2004;410:101–7. [https://doi.org/10.1016/S0040-6031\(03\)00401-5](https://doi.org/10.1016/S0040-6031(03)00401-5).
- [50] Szpak 1 S, Mosier-Boss 1 PA, Gordon 1 F, Dea 1 J, Miles 2 M, Khim 3 J, Forsley L. SPAWAR systems center-pacific Pd:D Co-deposition research: overview of refereed LENR publications. In: International Conference on Condensed Matter Nuclear Science (or International Conference on Cold Fusion ICCF). 14; 2008. Washington, DC, <https://www.lenr-canr.org/acrobat/SzpakSspawarsyst.pdf>.
- [51] Mosier-Boss PA, Forsley LP, Gordon FE. Overview of Pd/D Co-deposition. *J. Condensed Matter Nucl. Sci.* August 2019;29(1):34–40. <https://doi.org/10.1016/B978-0-12-815944-6.00002-6>.
- [52] Pamela A. Mosier-boss, Pd/D Co-deposition. ARPA-E Workshop on Low-Energy Nuclear Reactions October 2021;21–22. [https://arpa-e.energy.gov/sites/default/files/2021LENR\\_workshop\\_Boss.pdf](https://arpa-e.energy.gov/sites/default/files/2021LENR_workshop_Boss.pdf).
- [53] Freire LO, de Andrade DA. Preliminary survey on cold fusion: it's not pathological science and may require revision of nuclear theory. *J Electroanal Chem* 15 December 2021;903:115871. <https://doi.org/10.1016/j.jelechem.2021.115871>.